JOURNAL OF MAGNETIC RESONANCE **131,** 131–138 (1998)
ARTICLE NO. MN971332

A Three-Dimensional DOSY–HMQC Experiment for the High-Resolution Analysis of Complex Mixtures

Hervé Barjat,* Gareth A. Morris,*[,1] and Alistair G. Swanson†

**Department of Chemistry, University of Manchester, Oxford Road, Manchester M13 9PL, United Kingdom; and*
†Pfizer Central Research, Sandwich, Kent CT13 9NJ, United Kingdom

Received May 7, 1997; revised November 17, 1997

A three-dimensional experiment is described in which NMR signals are separated according to their proton chemical shift, ^{13}C chemical shift, and diffusion coefficient. The sequence is built up from a stimulated echo sequence with bipolar field gradient pulses and a conventional decoupled HMQC sequence. Results are presented for a model mixture of quinine, camphene, and geraniol in deuteriomethanol.

Key Words: **DOSY; HMQC; diffusion; mixture analysis.**

The analysis of complex mixtures has always played an important part in chemistry; in recent years this importance has if anything increased in such areas as drug discovery, natural product research, and the petrochemical and food industries. The combination of chromatographic separation techniques with NMR spectroscopy has developed rapidly over the past 10 to 15 years; more recently, DOSY (diffusion-ordered spectroscopy) (*1–8*) has established itself as a viable competitor for techniques such as HPLC NMR that are based on physical separation. DOSY uses pulsed field gradient spin echo experiments to encode information on diffusion rates into the intensities of NMR signals, allowing diffusion coefficients to be determined for individual resonances.

There are two principal regimes in which DOSY techniques find application. The first is in the analysis of mixtures, typically of macromolecules, that show poorly resolved NMR spectra but contain species with a broad range of diffusion coefficients. The inability to resolve discrete signals from individual molecular species means that the signal decays measured are composites containing a number of different superimposed decay curves corresponding to different diffusion coefficients. Although considerable effort has been devoted to the numerical problem of extracting the maximum possible information from such composite decays, the accuracy that can be obtained for the diffusion coefficients thus extracted is generally severely limited, so that when a 2D DOSY spectrum showing chemical shift versus diffusion coefficient is constructed from the NMR and diffusion data, it shows relatively poor resolution in both domains. In this regime, therefore, DOSY is most suitable for the low-resolution analysis of mixtures containing species of very different sizes (*4*).

In the second regime, by contrast, the ability to obtain resolved NMR signals from sharp lines (and by implication from small molecules) means that high resolution can also be obtained in the diffusion domain, because each signal shows only a single rather than a composite decay curve (*5, 7*). With suitable experimental and processing methods (*7*), relative accuracies as good as 0.2% can be obtained for the diffusion coefficients extracted from the spin echo experiments, and hence very good resolution can be obtained in the diffusion domain. This high-resolution variant of DOSY is thus a powerful experiment for the analysis of complex mixtures of small molecules with relatively similar sizes, such as are often encountered in natural product chemistry and in drug discovery, and in some biofluids.

The limits of high-resolution DOSY are defined by the need to obtain resolved signals from individual species, and by the signal-to-noise ratio of the data obtained. The problem of resolution is a pressing one in more complex mixtures, because of the relatively narrow range of proton chemical shifts. Various extensions to the basic proton DOSY experiment have been proposed, including polarization transfer to ^{13}C (*9, 10*), and the addition of a second NMR frequency domain to give 3D DOSY–NOESY (*11*), DOSY–COSY (*12, 13*), DOSY–DQS (*14*), or DOSY–TOCSY (*15*). Probably the highest information content available from a 3D DOSY experiment would be that from one combining proton and ^{13}C resolution, in order to benefit from the very high chemical shift dispersion that this would bring. This article describes such an experiment, in which a DOSY domain is added to the HMQC experiment.

In designing an experiment such as DOSY–HMQC, essentially a 3D NMR experiment with relatively few increments in the third (diffusion) dimension, experimental time becomes of crucial importance. The sequence should be designed to yield the desired information in as few phase cy-

[1] To whom correspondence should be addressed.

1090-7807/98 $25.00

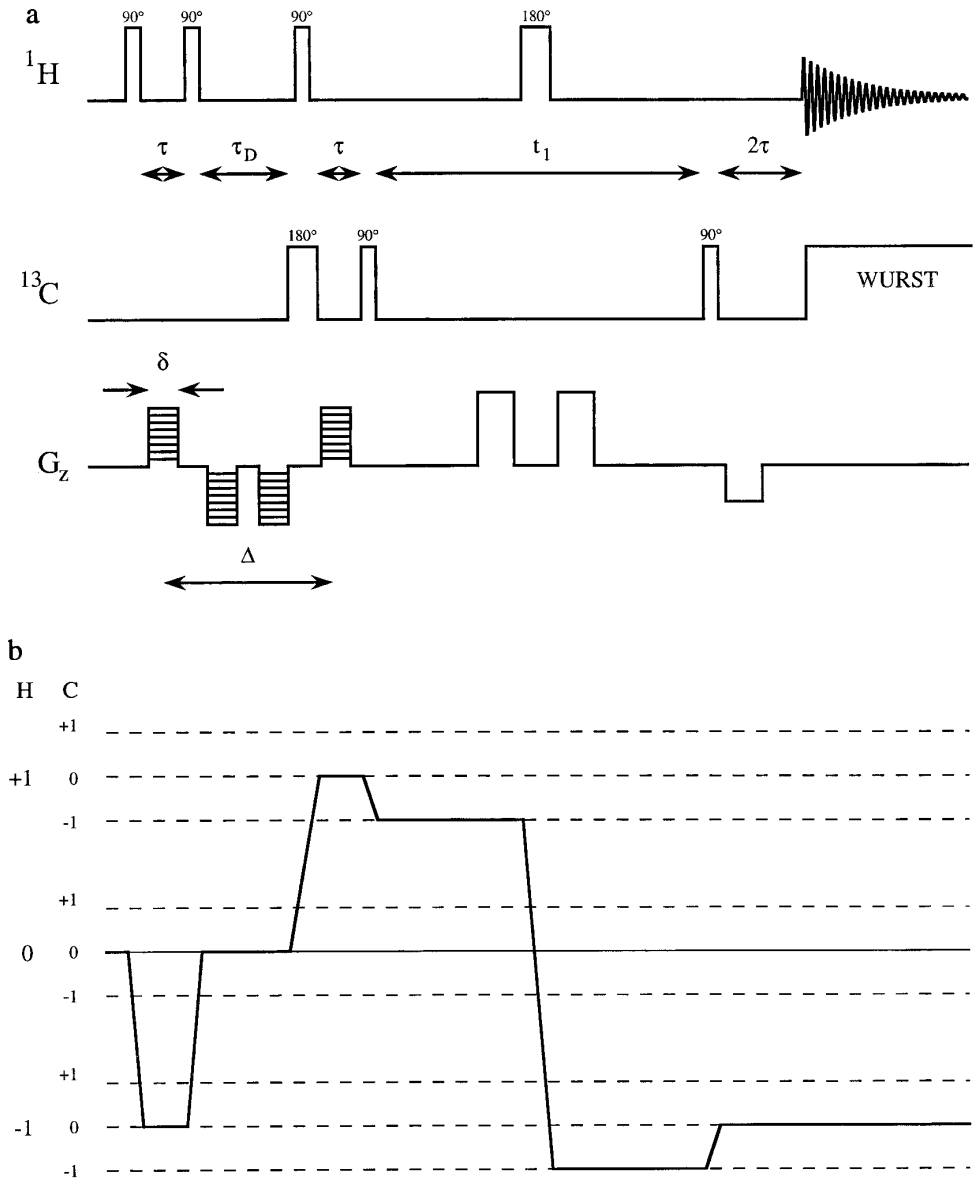

FIG. 1. (a) Pulse sequence for three-dimensional DOSY–HMQC and (b) coherence transfer pathway. The delays τ are of duration $1/(4^1J_{CH})$, and the variable diffusion encoding gradient pulses of strength G_Z^1 and width δ; the time between the midpoints of the outer variable gradient pulses is Δ. Limits on experiment duration allow only rudimentary phase cycling: the first ^{13}C 90° pulse follows the sequence $x, -x$ (02) on successive transients, the second proton 90° pulse $x, x, -x, -x, y, y, -y, -y$ (0022 1133), and the receiver $x, -x, -x, x, -y, y, y, -y$ (0220 3113).

cling steps as possible, so that the minimum experimental time needed is determined by the signal-to-noise ratio available from the sample rather than by the need to complete the phase cycle for each increment.

The proposed pulse sequence, shown in Fig. 1a, is divided into two main parts. It is a conventional gHMQC experiment (*16*) in which the delay after the first radiofrequency pulse has been replaced by a stimulated echo sequence with an additional ^{13}C 180° pulse. The coherence transfer pathway of the desired signal is shown in Fig. 1b. The diffusion encoding is accomplished using a three-pulse stimulated echo sequence with pulsed field gradients (*17*); the variable gradient pulses during the diffusion delay τ_D are optional, but serve to cancel to first order the perturbation of B_0 and the deuterium lock signal during the stimulated echo sequence, improving the f_1 lineshape in the final 3D spectrum. As well as providing time for the gradient pulses, the delays $\tau = 1/(4^1J_{CH})$, in conjunction with the 180° ^{13}C pulse, serve to bring the proton magnetization into an antiphase state with respect to one-bond couplings to ^{13}C at the maximum of the stimulated echo. The purpose of the 180° pulse is to introduce heteronuclear modulation into the stimulated echo, re-

moving the need for the initial 2τ delay in the HMQC segment of the sequence. If the area of the field gradient pulse required is so large that its duration must be greater than $1/(4^1J_{CH})$, then the 180° ^{13}C pulse can be omitted and a further delay $1/(2^1J_{CH})$ added between the stimulated echo midpoint and the first 90° ^{13}C pulse. In both cases the magnetization is transformed into heteronuclear zero- and double-quantum coherence by the first 90° carbon pulse, and from then on the basic gHMQC procedure is followed. The diffusion information is obtained by repeating the entire experiment for a number of diffusion encoding gradient strengths G_Z^1 (largely determined by the experimental time available) in the stimulated echo part of the experiment (see Fig. 1a), just as in the 2D DOSY experiment.

The minimum advisable phase cycling is of four steps, restricting the signals observed to those originating with the first pulse and experiencing the first ^{13}C 90° pulse; extending this to eight steps allows the addition of N-type coherence transfer pathway selection over the initial stimulated echo, which enables small values of the field gradient G_Z^1 to be used without interference from the unwanted *P*-type pathway. The eight-step phase cycling eliminates some undesirable coherence transfer pathways originating in the stimulated echo section of the sequence, for example, those proceeding via double-quantum coherence during the diffusion period τ_D or via the partial refocusing of one of the variable initial gradient pulses in the echo sequence by the fixed gradient pulses in the HMQC section of the sequence. Where more than eight transients are used the phase cycling can usefully be extended to include CYCLOPS.

Pulsed field gradients are used for the coherence selection in the HMQC part in order to minimize the effects of t_1 noise and to keep the number of phase cycling steps to a minimum. This produces much cleaner spectra and enables signals from minor components to be seen clearly without being obscured by t_1 noise from nearby intense proton resonances. This is particularly important for samples with a large dynamic range, as is often the case with complex mixtures. Although the experiments to be described here used absolute value presentation of the data, the DOSY–HMQC experiment may be carried out in phase-sensitive mode by combining data from experiments using *P*-type and *N*-type coherence transfer pathways for the HMQC section of the pulse sequence. Where the highest possible diffusion resolution is being sought, phase-sensitive display would be the method of choice, since the effect of noise contributions always being positive will be to introduce a small systematic error in the direction of increased diffusion coefficient.

Unlike previously reported 3D variants on DOSY, the DOSY–gHMQC experiment requires ^{13}C decoupling during the acquisition period. This introduces a new complication, and the choice of the method of decoupling turns out to be critical if reliable diffusion information is to be obtained. In this article, decoupling has been achieved using the broadband adiabatic WURST (*18*) method, even though the width of the ^{13}C spectrum on the 400-MHz (proton) spectrometer used would not be a problem for more conventional decoupling schemes. A ''cool'' decoupling method was favored here because even the relatively modest heat deposition in the sample using conventional decoupling schemes such as WALTZ or GARP-1 distorts the diffusion measurements. In ''normal'' HMQC experiments, small temperature disturbances are not particularly important, and can be dealt with by a period of steady-state transients prior to the start of the actual experiment. Unfortunately, this approach does not eliminate the problem in the DOSY–gHMQC experiment. The sample heating generates convection currents in the solution which have a dramatic effect on the apparent diffusion coefficients.

Because the pulsed field gradient used and the direction of convection are both oriented along the vertical (z) axis, even very slow convection currents will cause significant signal attenuation, and hence enhance the apparent rate of diffusion measured. The effects of convection have been discussed in the context of T_1 measurements (*19*), where sample spinning has been advocated as a possible solution, but unfortunately this is not viable where diffusion measurements are concerned. The maximum field gradient used here is about 30 G cm^{-1} and the diffusion delay τ_D of the order of 50 ms, so for an isochromat to dephase through one radian requires motion through a distance of the order of 0.25 μm in 50 ms. Thus significant signal attenuation will be caused by convection drift velocities of only a few micrometers per second (it is diverting to reflect that in the absence of diffusion, extending τ_D to 1 s would enable the effects of velocities of less than 10 nm s^{-1} to be detected—of the same order as the speed of continental drift). There is thus a pressing need to minimize the decoupling power used; WURST decoupling for ^{13}C enables high decoupling efficiency to be achieved (at the expense of some extra sidebands) with much lower powers than modulation schemes such as WALTZ and GARP. Under the experimental conditions used here, an average radiofrequency power during data acquisition of ca. 1 W proved sufficient. This greatly reduces the convection currents in the sample compared with comparable experiments using WALTZ modulation, restoring the measured diffusion coefficients to their ''true'' values.

No prior knowledge about the mixture is used in the processing. The extraction of diffusion coefficients from the 3D data set requires several steps, starting with a series of double Fourier transformations to give a 2D gHMQC spectrum for each value of G_Z^1. For the 2D spectrum with the lowest G_Z^1, the peak area regions are defined using standard NMR software; where possible, all the peaks for a given F_2 multiplet are included in a single area in order to maximize signal-to-noise ratio. The volume of each region is then evaluated for the corresponding regions in all the G_Z^1 increments, and

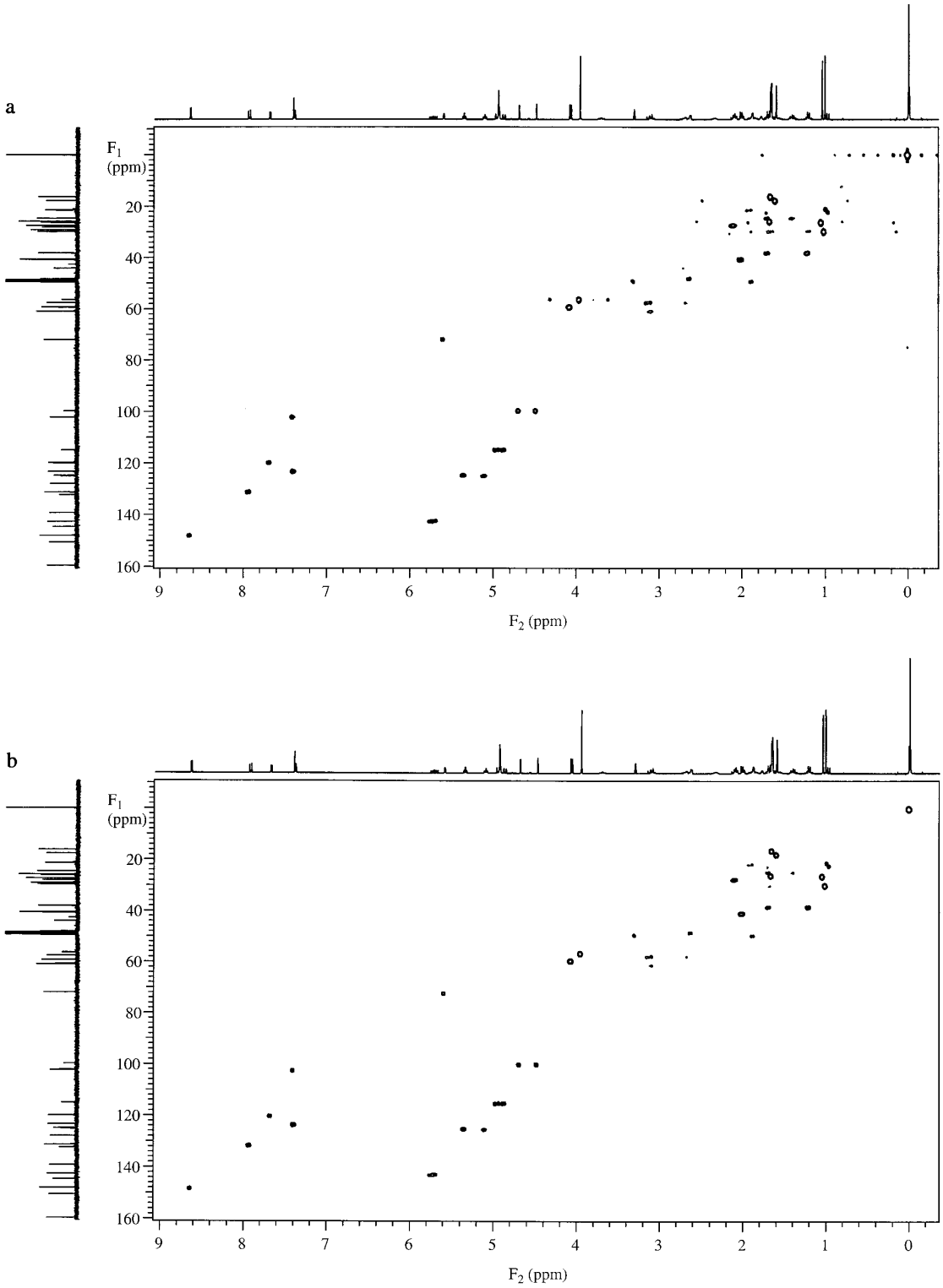

FIG. 2. HMQC spectrum of a mixture of quinine, camphene, geraniol, and TMS in deuteriomethanol. (a) The first 2D spectrum (low gradient strength) in a series acquired with the pulse sequence of Fig. 1a. Five 2D spectra were acquired with the sequence of Fig. 1a using field gradient pulses in the stimulated echo section of the sequence with widths of 1.54 ms, filling the delays τ, and strengths of 1, 15, 21, 26, and 30 G cm^{-1}. HMQC coherence transfer pathway selection was achieved with fixed gradient pulses of width 1.9 ms and strengths 10, 10, and -5 G cm^{-1}, respectively. For each 2D spectrum, 512 increments of four transients of 1024 complex points each were acquired, giving a total experimental time for the five 2D spectra of 17 h. Spectral widths of 20,455 and 4631 Hz were used in F_1 and F_2, respectively, and the data were processed using sine-bell weighting, zero filling in both dimensions, and absolute value display. (b) A ''normal'' gradient HMQC spectrum of the same mixture, acquired using the same experimental parameters. The main difference between spectra (a) and (b) is the presence in spectrum (a) of decoupling sidebands in F_2 produced by WURST, as a consequence of the very-low-power decoupling.

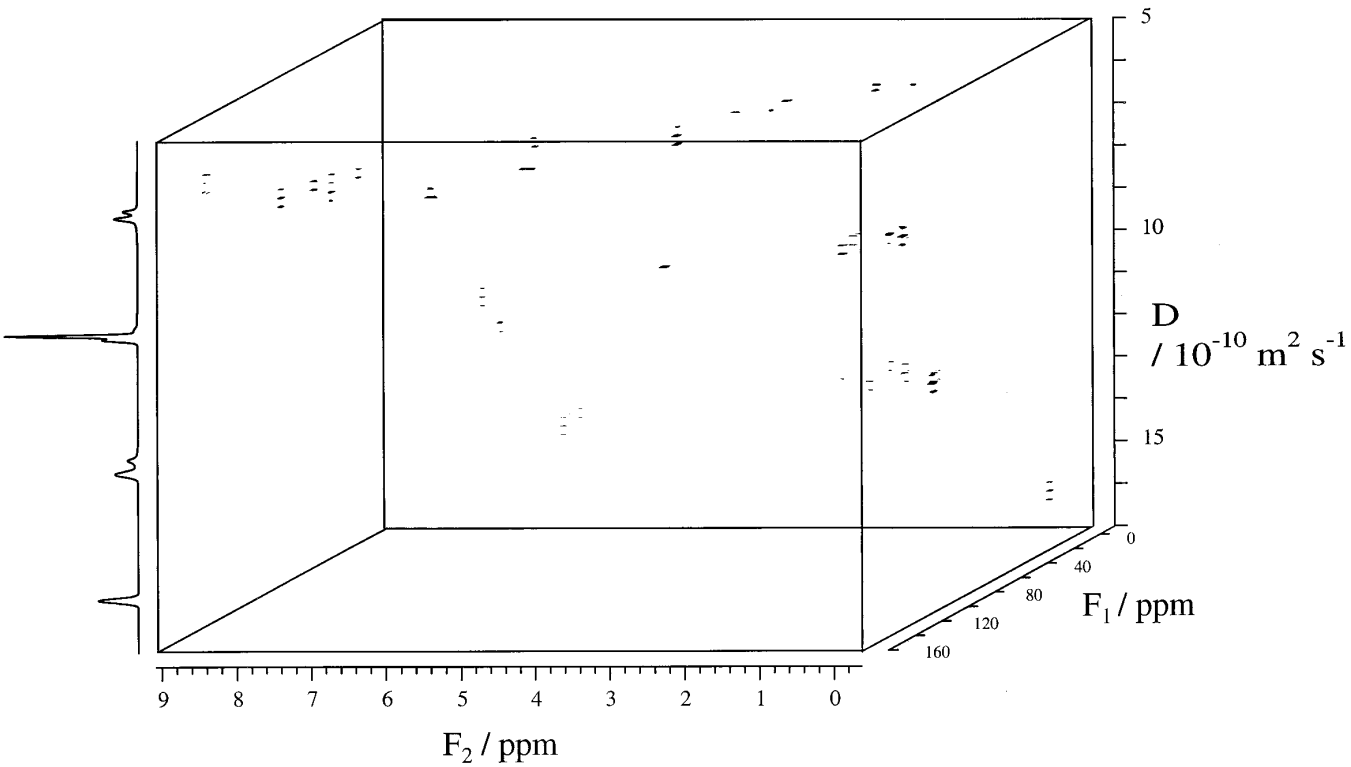

FIG. 3. 3D DOSY–HMQC spectrum of a mixture of quinine, camphene, and geraniol in deuteriomethanol, with (left) the integral projection onto the diffusion axis. The digitization in the diffusion domain has been restricted to 0.2×10^{-10} m^2 s^{-1} per point for ease of presentation.

an exponential least-squares fit of peak volume to the square of gradient area is carried out using the equation (*20*)

$$S(G_{zi}^1) = S_0 \exp(\gamma^2 \delta^2 (G_{zi}^1)^2 (\Delta - \delta/3)),$$

where δ is the width of the variable gradient pulses and Δ the separation between their midpoints. Each peak area is thus assigned a diffusion coefficient and a corresponding standard error estimated from the fitting statistics. A 3D DOSY spectrum can then be constructed by taking the 2D peak shape for each signal in turn from the 2D spectrum for lowest G_Z^1 and convoluting it in the third dimension with a Gaussian lineshape centered on the fitted diffusion coefficient and with a width determined by the standard error, but in practice a full 3D display is of limited value.

A simpler way of visualizing the results is to construct the integral of the 3D spectrum between given limits in the diffusion domain, by editing the 2D HMQC spectrum for the weakest G_Z^1 so as to display only that portion of the signal that falls within a chosen diffusion region; the result is thus a diffusion-edited HMQC spectrum. This is achieved by using a modified version of the existing Vnmr software, giving the display of a projection of a slab of the 3D data set, at a selectable diffusion value and of a selectable thickness, onto the HMQC plane. It is thus possible to extract the HMQC spectra of the individual components of a mixture on the basis of the diffusion information. The total processing time, once the peak regions have been defined, is effectively the same as that for the series of 2D Fourier transformations; on the Sparc 5 clone used, a single 2D transformation (of 2K $\times$ 1K complex points) took 1 min 41 s, and the complete DOSY analysis using all five datasets 8 min 22 s. The time needed for the display of a given diffusion region, 57 s on this system, is determined largely by the short time needed to copy the 2D spectral display to disk. At no stage in the process is there a need for a large data transfer or change in data format, so the entire operation is simple and rapid.

The DOSY–gHMQC experiment was tested at room temperature on a sample containing quinine (30 mg), geraniol (20 μl), camphene (19 mg), and TMS in deuteriated methanol, using the 5-mm indirect detection PFG probe of a Varian Associates INOVA 400 spectrometer. The duration of the diffusion delay τ_D in the stimulated echo part of the sequence was kept short (43 ms) in order to avoid excessive signal loss through T_1 relaxation. HMQC data were acquired for five increments of G_Z^1, in a total experiment time of 17 h. Appropriate values of G_Z^1 for this longitudinal delay were found by performing a quick experiment with a single t_1 increment and looking for a maximum signal attenuation of

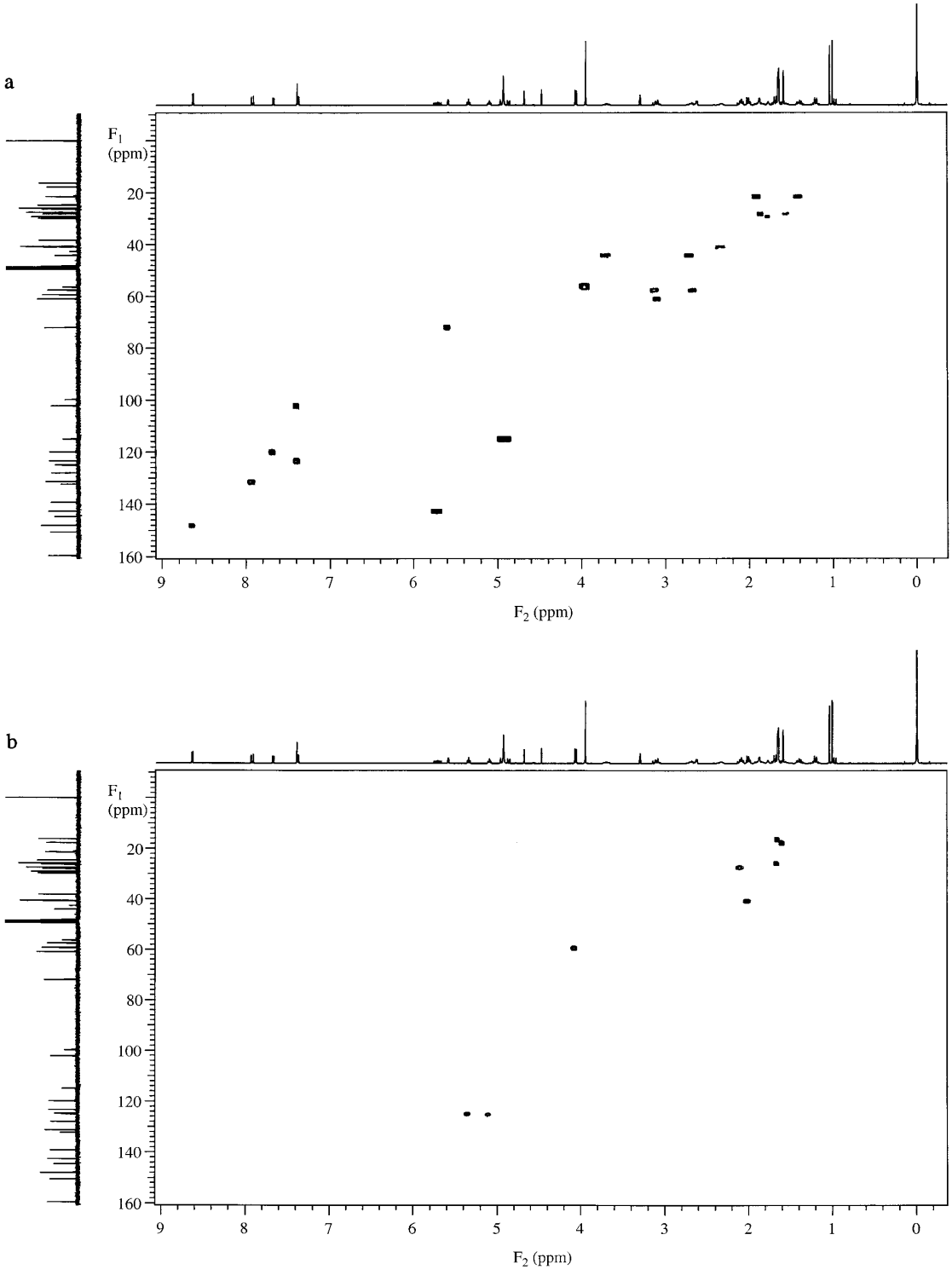

FIG. 4. 2D projections of the 3D DOSY–HMQC spectrum of a mixture of quinine, camphene, and geraniol in deuteriomethanol onto the HMQC plane, for diffusion coefficient limits of (a) 5.9–6.9 $\times$ 10^{-10} m^2 s^{-1}, (b) 9.0–10.0 $\times$ 10^{-10} m^2 s^{-1}, and (c) 12.1–13.1 $\times$ 10^{-10} m^2 s^{-1}, showing the resolved HMQC spectra of the quinine, geraniol, and camphene, respectively.

ca. 70–80% between the weakest and strongest gradient. The recycle time was set to a conservatively large value in order to keep the decoupler duty cycle to a minimum.

Figure 2a shows the gHMQC spectrum obtained for the lowest value of G_Z^1, and for comparison purposes Fig. 2b shows a conventional gradient HMQC spectrum of the mix-

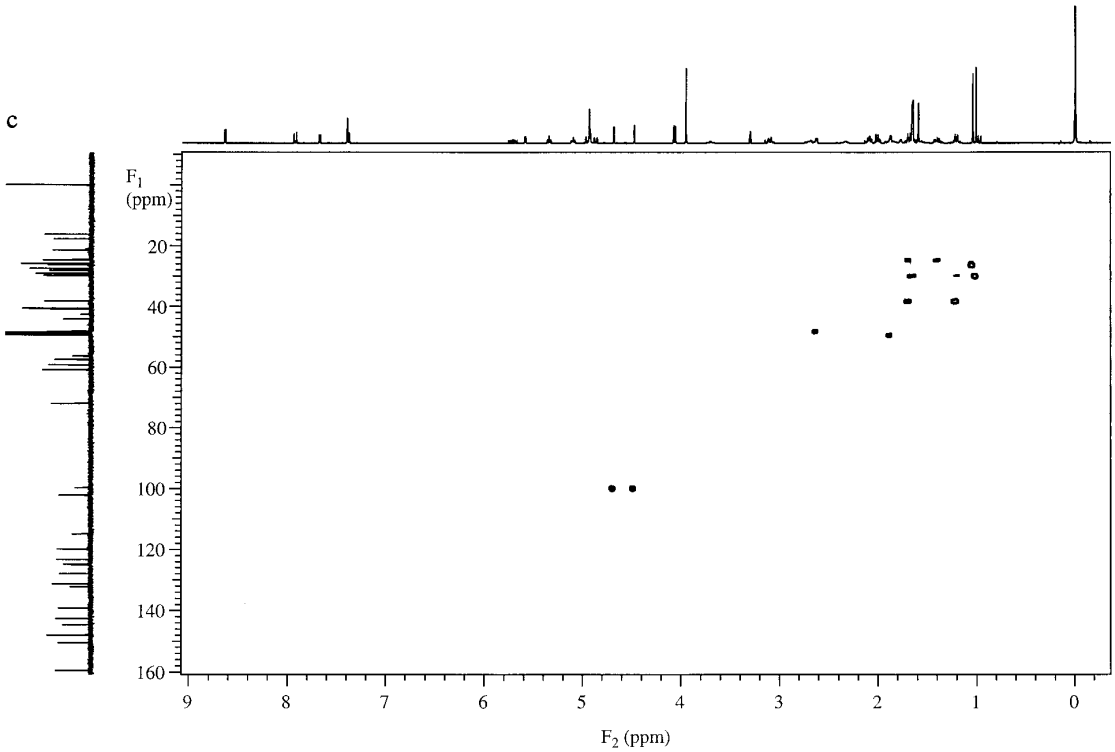

FIG. 4—*Continued*

ture acquired with WALTZ ^{13}C decoupling. The main difference between the two 2D spectra, apart from slight changes in relative signal intensities due to the extra signal evolution during the initial stages of the DOSY–gHMQC sequence, is the presence of decoupling sidebands attributable to the WURST decoupling at low power. Since the present software uses manual identification of the areas for peak integration, the WURST cycling sidebands do not represent a significant problem, but in the most complex mixtures there is scope for seeking further improvements in the decoupling modulation scheme. Figure 3 shows the full 3D spectrum, constructed directly from the diffusion coefficients, standard errors, and initial peak volumes, and its projection onto the diffusion axis. The four components of the mixture are clearly separated, although several cross peaks that partially overlap in both ^{1}H and ^{13}C dimensions give rise to diffusion coefficients which differ slightly from those found for well-resolved signals; these cross peaks are responsible for the ''satellite'' peaks seen to one or other side of the main diffusion peak for each species in the diffusion projection at the left-hand side of Fig. 3. Figure 4a shows a projection of the 3D data set onto the HMQC plane for the region between $D = 5.9 \times 10^{-10}$ and 6.9×10^{-10} m^2 s^{-1}, showing only signals from quinine. Figure 4b shows the corresponding projection for the region $D = 9.0 \times 10^{-10}$ to 10.0×10^{-10} m^2 s^{-1}, containing only geraniol signals, and Figure 4c the projection for camphene, covering the region $D = 12.1 \times 10^{-10}$ to 13.1×10^{-10} m^2 s^{-1}.

The data presented illustrate the powerful separation possibilities of the DOSY–gHMQC experiment. The principal limitation of the technique is imposed by the natural abundance of ^{13}C, which limits the signal-to-noise ratio obtainable in the HMQC experiment and hence the quality of the diffusion information obtainable. An examination of the experimental data shows a clear inverse correlation between standard error of diffusion coefficient and peak volume, suggesting that the principal limitation on the quality of the diffusion data is that set by the random errors caused by spectral noise. This limitation can be overcome by using higher magnetic fields or better probe designs offering more sensitivity (such as microprobes), as well as by increasing the number of transients per increment. Smaller but still worthwhile improvements in sensitivity and resolution could be obtained by the use of phase-sensitive processing, and by replacing the HMQC sequence by the sensitivity-enhanced HSQC sequence of Kay *et al.* (*21*).

As is the case in many branches of spectroscopy, the best choice of a DOSY experiment depends on the compromise required between sensitivity and resolution. The DOSY–gHMQC experiment offers what is currently the highest spectral resolution of any DOSY technique, and conversely one of the lowest sensitivities, and would appear to be the method of choice for very complex mixtures with high concentrations. It poses some interesting instrumental problems, most notably the need for extremely efficient heteronuclear decoupling if problems caused by very slow convection currents are to be avoided.

ACKNOWLEDGMENTS

The support of the EPSRC (Grants GR/K16296, GR/K44619, and GR/L17443) is gratefully acknowledged, as is support from Pfizer Central Research, Sandwich. G.A.M. thanks the Leverhulme Trust for a Research Fellowship.

REFERENCES

1. P. Stilbs, *Anal. Chem.* **53,** 2135 (1981).
2. K. F. Morris and C. S. Johnson, Jr., *J. Am. Chem. Soc.* **114,** 3139 (1992).
3. K. F. Morris and C. S. Johnson, Jr., *J. Am. Chem. Soc.* **115,** 4291 (1993).
4. D. P. Hinton and C. S. Johnson, Jr., *J. Phys. Chem.* **97,** 9064 (1993).
5. D. H. Wu, W. S. Woodward, and C. S. Johnson, *J. Magn. Reson. A* **104,** 231 (1993).
6. K. F. Morris, P. Stilbs, and C. S. Johnson, *Anal. Chem.* **66,** 211 (1994).
7. H. Barjat, G. A. Morris, S. Smart, A. G. Swanson, and S. C. R. Williams, *J. Magn. Reson. B* **108,** 170 (1995).
8. G. A. Morris, *in* ''Methods for Structure Elucidation by High Resolution NMR'' (G. Batta and K. Köver, Eds.), Elsevier, Amsterdam (1997).
9. D. H. Wu, A. D. Chen, and C. S. Johnson, *J. Magn. Reson. A* **123,** 215 (1996).
10. G. A. Morris, 12th International NMR Meeting, Royal Society of Chemistry, Manchester, United Kingdom (1995).
11. E. K. Gozansky and D. G. Gorenstein, *J. Magn. Reson. B* **111,** 94 (1996).
12. D. H. Wu, A. D. Chen, and C. S. Johnson, *J. Magn. Reson. A* **121,** 88 (1996).
13. H. Barjat, G. A. Morris, and A. G. Swanson, 13th European Experimental NMR Conference, Paris, France (1996).
14. N. Birlirakis and E. Guittet, 13th European Experimental NMR Conference, Paris, France (1996).
15. N. Birlirakis and E. Guittet, *J. Am. Chem. Soc.* **118,** 13083 (1996).
16. J. Ruiz-Cabello, G. W. Vuister, C. T. W. van Moonen, P. van Gelderen, J. S. Cohen, and P. C. M. van Zijl, *J. Magn. Reson.* **100,** 282 (1992).
17. D. H. Wu, A. D. Chen, and C. S. Johnson, *J. Magn. Reson. A* **115,** 260 (1995).
18. Ē. Kupče and R. Freeman, *J. Magn. Reson. A* **118,** 299 (1996).
19. J. Lounila, K. Oikarinen, P. Ingman, and J. Jokisaari, *J. Magn. Reson. A* **118,** 50 (1996).
20. E. O. Stejskal and J. E. Tanner, *J. Chem. Phys.* **42,** 288 (1965).
21. L. E. Kay, P. Keifer, and T. Saarinen, *J. Am. Chem. Soc.* **114,** 10663 (1992).